





Original Article


## Use of $^{137}\text{Cs}$ and $^{210}\text{Pb}_{\text{ex}}$ fallout radionuclides for spatial soil erosion and redistribution assessment on steeply sloping agricultural highlands



Jung-Hwan YOON<sup>1,2</sup>  <https://orcid.org/0000-0001-8009-7807>; e-mail: yoonfnfg@hanmail.net

Young-Nam KIM<sup>3</sup>  <https://orcid.org/0000-0002-9745-6551>; e-mail: youngnam.a.kim@gmail.com

Kye-Hoon KIM<sup>4</sup>  <https://orcid.org/0000-0002-4891-3322>; e-mail: johnkim@uos.ac.kr

M.B. KIRKHAM<sup>5</sup>  <https://orcid.org/0000-0001-9518-3548>; e-mail: kirkhammb@gmail.com

Hyuck Soo KIM<sup>2</sup>  <https://orcid.org/0000-0001-9944-6245>; e-mail: kimhs25@kangwon.ac.kr

Jae E. YANG<sup>2\*</sup>  <https://orcid.org/0000-0001-8641-6442>;  e-mail: yangjay@kangwon.ac.kr

\*Corresponding author

<sup>1</sup> Kangwon Institute of Inclusive Technology, Kangwon National University, Chuncheon 24341, Republic of Korea

<sup>2</sup> Department of Biological Environment, Kangwon National University, Chuncheon 24341, Republic of Korea

<sup>3</sup> Institute of Agriculture and Life Science, Gyeongsang National University, Jinju 52828, Republic of Korea

<sup>4</sup> Department of Environmental Horticulture, University of Seoul, Seoul 02504, Republic of Korea

<sup>5</sup> Department of Agronomy, Kansas State University, Manhattan, KS 66506-0110, USA

**Citation:** Yoon JH, Kim YN, Kim KH, et al. (2021) Use of  $^{137}\text{Cs}$  and  $^{210}\text{Pb}_{\text{ex}}$  fallout radionuclides for spatial soil erosion and redistribution assessment on steeply sloping agricultural highlands. *Journal of Mountain Science* 18(11). <https://doi.org/10.1007/s11629-021-7080-0>

© Science Press, Institute of Mountain Hazards and Environment, CAS and Springer-Verlag GmbH Germany, part of Springer Nature 2021

**Abstract:** The steeply sloping agricultural highlands in Korea have severe soil erosion. Estimation of both soil erosion and sedimentation in these highlands is necessary to make plans for soil-conservation measures, but it is not feasible using existing soil-erosion models. This study measured the site-specific concentrations of  $^{137}\text{Cs}$  and  $^{210}\text{Pb}_{\text{ex}}$  on both a highland slope (33% slope) and a reference site (undisturbed flat area) to estimate soil erosion and redistribution. The use of the fallout radionuclide (FRN) method was evaluated to see if it is a suitable method for characterizing soil erosion. Results were compared with those obtained with the Universal Soil Loss Equation (USLE), which is an empirical model that estimates annual soil erosion. The average concentrations of  $^{137}\text{Cs}$  and  $^{210}\text{Pb}_{\text{ex}}$  at the reference site

were  $11.57 \pm 0.24$  Bq  $\text{kg}^{-1}$  and  $59.74 \pm 4.2$  Bq  $\text{kg}^{-1}$ , respectively. Concentrations of  $^{137}\text{Cs}$  and  $^{210}\text{Pb}_{\text{ex}}$  in the experimental slope were 16.4% and 10.8%, respectively, of those at the reference site. Radionuclide inventories were lower at the upper point of the slope than those at the basal point of the slope. Concentrations of  $^{137}\text{Cs}$  and  $^{210}\text{Pb}_{\text{ex}}$  were significantly correlated with available phosphorus, organic matter, CEC, and exchangeable cations. Estimation of soil redistribution rate using  $^{137}\text{Cs}$  and  $^{210}\text{Pb}_{\text{ex}}$  showed site-specific variations at different points along the slope, and respective ranges were  $-17.46 \sim -207.51$  and  $1.55 \sim -581.38$  Mg  $\text{ha}^{-1}$   $\text{yr}^{-1}$ , which indicated that more erosion was assessed by  $^{210}\text{Pb}_{\text{ex}}$  than by  $^{137}\text{Cs}$ . Redistribution analysis showed that soil erosion occurred along the entire slope, except for the bottom point of the slope where 1.55 Mg  $\text{ha}^{-1}$   $\text{yr}^{-1}$  of sediment accumulated. The USLE provided a single value of the average annual soil loss in the entire slope,

**Received:** 31-Aug-2021

**Revised:** 28-Sep-2021

**Accepted:** 08-Oct-2021

which was either 166 or 398 Mg ha<sup>-1</sup> yr<sup>-1</sup>, depending on the soil erodibility factor (soil series factor and calculated factor from soil sample analysis) used in the model. We conclude that the FRN method using <sup>137</sup>Cs and <sup>210</sup>Pb<sub>ex</sub> radionuclides can be used to assess soil erosion and redistribution in steeply sloping agricultural highlands. Verification of soil-erosion values using the FRN method and soil-erosion models has been controversial, but it merits further study at many locations with different soils, topography, and management practices.

**Keywords:** Soil erosion; Steep highland; Fallout radionuclide; <sup>137</sup>Cs; <sup>210</sup>Pb<sub>ex</sub>; USLE

## 1 Introduction

Over the past several decades, a number of soil-erosion models that can predict generation, fate, and transport of sediment within a designated field or catchment have been developed to address a wide range of agronomic and environmental issues (Ascough II et al. 2018). Soil-erosion models can be classified into empirical and process-based models (Karydas et al. 2012). The empirical models, such as the Universal Soil Loss Equation (USLE: Wischmeier and Smith 1978) and the Revised Universal Soil Loss Equation (RUSLE: Renard et al. 1997), are used for on-site, field-scale assessment of soil erosion. These models have mostly been used for prediction of soil erosion in arable lands in Korea (Jung et al. 2004). Many process-based models, such as the Soil and Water Assessment Tool (SWAT) (Arnold et al. 1998), European Soil Erosion Model (EUROSEM) (Morgan et al. 1990), and the Water Erosion Prediction Project (WEPP) (Nearing et al. 1989; Flanagan et al. 2007), are frequently used for both on-site and off-site field-to watershed-scale assessments of management practices (Ascough II et al. 2018).

Soil-erosion models are mathematical procedures and estimate the potential for dislocation of sediment at the field or watershed level. Because models have varying levels of complexity and limitations depending upon soil, weather, topography, and land uses, the estimated soil-erosion values can fluctuate significantly among erosion models, even though they employ the same variables (Ascough II et al. 2018). Also, quantitative determination of spatial variability of erosion and sedimentation in a field using these models is not feasible (Croke and Nethery

2006; Mabit et al. 2008). Soil-erosion measurements on very steep slopes using existing models, such as USLE, are erratic and cost-ineffective due to many factors (Jung et al. 2004; Jung et al. 2015; Park et al. 2004). On sloping agricultural highlands, which are subject to high amounts soil erosion due to continuous cropping, assessments of both soil erosion and redistribution are critically needed for soil-conservation plans.

As an alternative to the models cited above, a method based on fallout radionuclides (FRNs) has been used for soil-erosion research in many parts of the world (An et al. 2014; Arata et al. 2016; IAEA 2014; Mabit et al. 2009, 2018; Meusburger et al. 2020; Quijano et al. 2016; Ritchie and McHenry 1990; Zapata 2002). The radioisotopes used for FRNs are artificial radioactive cesium-137 (<sup>137</sup>Cs) and natural radioactive excess lead-210 (<sup>210</sup>Pb<sub>ex</sub>) that have half-lives of 30.2 and 22.3 years, respectively. The <sup>210</sup>Pb<sub>ex</sub> is the difference between total and indigenous Pb radioactive concentration in soil (He and Walling 1997; IAEA 2014; Mabit et al. 2014; Walling et al. 2007). Initially, the radionuclides are deposited uniformly on the ground surface with rainfall and subsequently bind strongly with soil particles (Mabit et al. 2008). Consequently, a significant correlation between quantity of soil loss and reduction in <sup>137</sup>Cs and <sup>210</sup>Pb<sub>ex</sub> has been found in various soil-erosion studies (Rabesiranana et al. 2016; Ritchie and McHenry 1990; Zapata 2002). Soil-erosion research using FRNs was initiated in the 1950s to 1960s, mostly as a result of <sup>137</sup>Cs fallout from testing of global nuclear weapons. Since then, the activity of <sup>137</sup>Cs in soil has decreased due to its half-life (30.2 years) and <sup>210</sup>Pb<sub>ex</sub> has been substituted for <sup>137</sup>Cs, because it has a behavior similar to that of <sup>137</sup>Cs in soil (IAEA 2014; Mabit et al. 2008, 2018).

About 10% of the total upland acreage in Korea is located in alpine regions with elevations higher than 600 m above sea level. In these alpine lands, cash crops, such as cabbage, radish, and potato, are produced mainly during the summer season when temperatures support growth. About 60% of the alpine lands are classified in a steep-slope class, which has slopes greater than 15%. Slope lengths are long, stretched out, and undulating. This formation, in most cases, results in soil erosion occurring on some parts of the sloping surfaces but sedimentation occurring in other parts. This hinders implementation of best management practices for soil-erosion control

(Lee et al. 2010; MoE 2004). Most precipitation occurs during the summer monsoon season, and, thus, severe soil erosion exceeding 50 MT ha<sup>-1</sup> yr<sup>-1</sup> is inevitable in these alpine lands, which results in a reduction of vegetable production and an increase in loadings of nonpoint-source nutrient pollutants into river basins (Joo et al. 2004; Jung et al. 2015; Park et al. 2004; Park et al. 2011). Quantitative measurement of actual soil erosion and sedimentation in the steep highlands is an important step for designing sustainable conservation plans and, thereafter, for assessing the effects of agricultural conservation practices on crop production and environmental quality. Information on the combined use of FRNs and existing soil-erosion models for assessing soil erosion and redistribution in highlands with slopes greater than 30% is very limited.

The use of FRNs for soil erosion and sedimentation research is considered to be a more suitable method than use of various erosion models (Arata et al. 2016; Elliott et al. 1990; IAEA 2014; Mabit et al. 2002, 2008, 2018; Meusburger et al. 2020; Saç et al. 2008; Zapata 2002). However, studies to differentiate between soil erosion and sedimentation using FRNs, even within the same field, are limited. For example, Meusburger et al. (2013) employed a stable isotope and fallout radionuclides as soil-erosion indicators in forested sites but did not provide information concerning soil redistribution on slopes. The objectives of this study were (1) to assess the spatial distribution of <sup>137</sup>Cs and <sup>210</sup>Pb<sub>ex</sub> in soil profiles and on slopes, because these spatial data reflect the change of soil properties and soil-erosion

characteristics, (2) to assess the estimated amount of soil loss using FRNs and compare it's relevance to that by USLE, and (3) to investigate the feasibility of the FRN method in characterizing spatial soil erosion and redistribution in steeply sloping agricultural highlands.

## 2 Materials and Methods

### 2.1 Field site and soil sampling

The experimental site for assessing soil erosion and sedimentation was Anbandegi, a village located in the northeast of Gangwon Province, the Republic of Korea (Fig. 1). This site originally was a forested area, but it was reclaimed in the late 1960s for intensive production of vegetables, such as Chinese cabbage, radish, and potato, during the summer. This region is Korea's largest highland agricultural area and has the highest rate of soil erosion. The field site was located near the top of a mountain over 1,000 m above sea level, and it had an area of 11,000 m<sup>2</sup>, of which an area of 120 m × 20 m (L × W) in the middle of the field site was selected for the survey (Fig. 1). The site is classified as 'severely steep' with a 33% slope gradient. The field site is used for Chinese cabbage production. The long-term average annual temperature and precipitation are 6.6°C and 1,898 mm, respectively.

The locations where soil samples at the Anbandegi site were taken are shown in Fig. 1. A total of 21 soil samples (3 columns × 7 rows) were collected.

For uniformity, three subsamples at each point were taken and then combined. Additionally, five soil samples (1~2 m interval) were taken from a reference site (37°36'55.2"N, 128°44'11.6"E) on an undisturbed flat area adjacent to the experimental field site. The radioactivity of <sup>137</sup>Cs and <sup>210</sup>Pb<sub>ex</sub> at the reference site was used as the basis for soil-erosion estimation. All soil samples were taken to the 30-cm depth using a Cobra sampler (Cobra-248, Atlas Copco, Nacka, Sweden; core size 8.9 cm) to minimize soil disturbance. However, sampling depth at B7 site

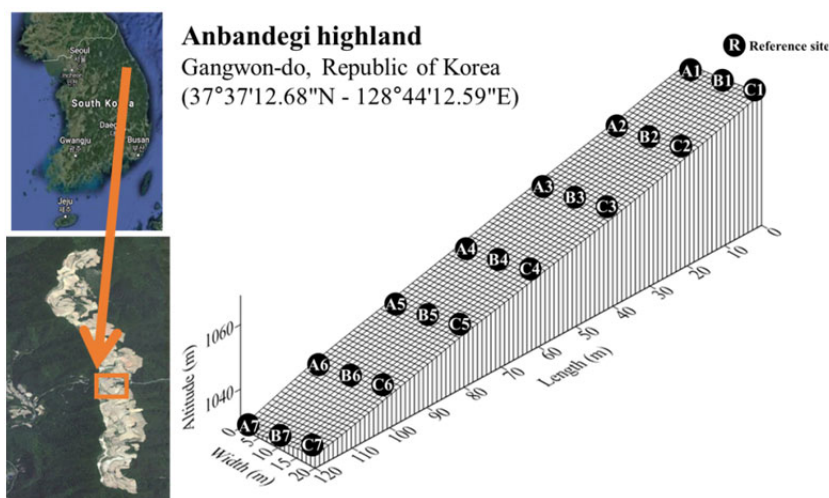


**Fig. 1** Location of the highland experimental site at Anbandegi and soil sampling points.

was up to 50 cm in order to see the detailed distribution of FRN.

## 2.2 Analysis of soil properties

Soil samples were air-dried and passed through a 2-mm sieve for chemical analyses. Soil pH and electrical conductivity (EC) were measured with a pH meter (MP 220, Mettler, Greifensee, Switzerland) and an EC meter (MC 226, Mettler, Greifensee, Switzerland), respectively. Available P in soil was determined using the Bray No. 1 method (Bray and Kurtz 1945). Soil organic matter content was analyzed by the Walkley-Black method (Nelson and Sommers 1996). Exchangeable cations and cation exchange capacity (CEC) were determined using 1 M ammonium acetate saturation and N distillation apparatus (Kjeltec 2300, Foss, Hoganas, Sweden) (Sumner and Miller, 1996). Soil texture was determined using the micro-pipette method (Miller and Miller 1987).

Average soil pH of the Anbandegi highland was 5.33, and pH varied with the sampling points (Table 1). The pH was lower in the upper parts of the slope than in the lower parts. This trend corresponded with changes of EC, available P, organic matter,

exchangeable cations, and CEC. Soil texture in the upper parts of the field site was coarser than that in the lower parts. These changes might be due to the continuous soil erosion on the steep slopes. Mabit and Bernad (1998) reported similar trends in soil-property changes.

## 2.3 Concentration and inventory of $^{137}\text{Cs}$ and $^{210}\text{Pb}_{\text{ex}}$ in soil

To measure the radioactivity of  $^{137}\text{Cs}$ ,  $^{210}\text{Pb}$ , and  $^{226}\text{Ra}$  in soil, 0.5 L Marinelli beakers were filled with soil samples, weighed, and completely sealed. For measuring the radioactivity of  $^{226}\text{Ra}$ , the radioactive decay products of  $^{214}\text{Pb}$  and  $^{226}\text{Ra}$  were left to reach radioactive equilibrium for 20 days in the 0.5 L Marinelli beakers. The gamma-ray energy spectrum of the soil was then measured for 80,000 seconds using an energy extended low energy gamma-ray spectrometer (Broad Energy HPGe detector, Canberra Model BE5030-7915-30/ULB, Meriden, CT, USA). Activities of  $^{210}\text{Pb}$ ,  $^{137}\text{Cs}$ , and  $^{214}\text{Pb}$  were determined from the gamma ray peaks at 46.5 keV, 662 keV, and 352 keV, respectively. Total  $^{210}\text{Pb}$  measured at the 46.5 keV peak was the sum of the indigenous  $^{210}\text{Pb}$  generated on-site and  $^{210}\text{Pb}$  incorporated from

**Table 1** Soil physicochemical properties of twenty-one samples from the Anbandegi highland. See Fig. 1 for the locations of the sampling points.

Sampling point	pH (1:5W)	EC (dS m <sup>-1</sup> )	Avail.P (mg kg <sup>-1</sup> )	OM (%)	CEC (cmol kg <sup>-1</sup> )	Ca	Mg	K	Sand (%)	Silt (%)	Clay (%)	Texture
A1	5.17	0.08	196.3	1.94	12.5	1.7	0.7	0.8	49.4	43.9	6.7	Sandy loam
A2	5.91	0.13	187.9	3.23	14.5	4.4	1.2	0.9	40.4	50.2	9.4	Silt loam
A3	5.47	0.14	216.8	4.08	17.6	3.4	1.2	1.1	32.9	58.4	8.7	Silt loam
A4	5.13	0.13	192.4	5.27	21.5	3.1	1.0	1.0	29.9	60.8	9.3	Silt loam
A5	5.42	0.08	361.7	1.97	19.1	2.7	1.2	1.2	37.8	53.4	8.9	Silt loam
A6	5.39	0.11	309.8	5.82	22.3	3.6	1.2	1.1	33.7	57.1	9.2	Silt loam
A7	6.29	0.13	448.6	5.69	22.8	6.2	2.7	1.8	35.5	56.5	8.0	Silt loam
B1	5.2	0.09	172.6	1.67	12.5	1.8	0.7	0.6	45.6	47.4	7.0	Loam
B2	5.13	0.11	259.0	2.08	14.5	2.0	0.9	0.7	43.8	48.9	7.4	Loam
B3	5.05	0.10	264.6	6.02	17.7	1.9	0.6	0.8	34.9	54.7	10.4	Silt loam
B4	5.44	0.15	652.5	5.68	21.4	3.8	1.4	1.4	35.5	57.0	7.5	Silt loam
B5	5.17	0.07	79.5	2.52	13.1	1.5	0.4	0.6	39.9	52.2	8.0	Silt loam
B6	4.83	0.10	400.4	4.93	20.4	1.9	0.8	0.9	36.7	55.3	8.0	Silt loam
B7	6.04	0.16	515.9	4.78	19.0	5.1	1.6	1.4	41.0	51.7	7.3	Silt loam
C1	4.94	0.11	130.3	2.45	13.6	1.2	0.5	0.6	41.0	49.7	9.3	Loam
C2	5.22	0.12	163.6	3.71	16.9	2.2	0.8	0.9	36.7	52.8	10.5	Silt loam
C3	5.51	0.09	237.2	2.62	14.1	2.2	0.9	0.9	38.7	52.4	8.9	Silt loam
C4	5.35	0.12	153.6	3.23	16.1	2.5	0.7	0.9	38.0	54.0	8.0	Silt loam
C5	5.03	0.13	168.7	3.98	17.8	1.9	0.8	0.7	35.5	53.8	10.7	Silt loam
C6	5.03	0.16	109.9	3.91	16.7	2.0	0.7	0.8	33.3	56.3	10.4	Silt loam
C7	5.19	0.15	117.2	3.71	16.5	2.2	0.8	1.0	29.4	58.6	12.0	Silt loam
Average	5.33	0.12	254.2	3.78	17.17	2.7	1.0	1.0	37.6	53.6	8.8	-

**Note:** EC, electrical conductivity; Avail.P, Available Phosphorus; OM, organic matter; CEC, cation exchange capacity.

external sources. Because the indigenous  $^{210}\text{Pb}$  radioactivity is the same as that calculated from  $^{226}\text{Ra}$ , the fallout  $^{210}\text{Pb}_{\text{ex}}$  activity introduced from external sources was obtained by subtracting the radioactivity of  $^{226}\text{Ra}$  from total  $^{210}\text{Pb}$  (Eq. 1). The detection limit for  $^{137}\text{Cs}$  and  $^{210}\text{Pb}_{\text{ex}}$  measurements was 0.15 Bq/kg. Concentrations of  $^{137}\text{Cs}$  and  $^{210}\text{Pb}_{\text{ex}}$  were converted to the inventories of the respective radionuclides taking into consideration soil bulk density.

$$^{210}\text{Pb}_{\text{ex}} = \text{Total } ^{210}\text{Pb} - ^{226}\text{Ra} \quad (1)$$

## 2.4 Estimation of soil erosion rate using FRNs

The quantity of soil erosion (R value in Eq. 2) at the Anbandegi highland site, determined using  $^{137}\text{Cs}$  and  $^{210}\text{Pb}_{\text{ex}}$ , was estimated based on the differences in FRNs inventories between the reference area (flat area) and the slopes. To do this, the calculated radioactivity of  $^{137}\text{Cs}$  and  $^{210}\text{Pb}_{\text{ex}}$  was incorporated into the following mass balance model (Eq. 2) for soil erosion estimation (An et al. 2014; He and Walling 1997; Walling et al. 2007; Zapata 2002).

$$\frac{dA(t)}{dt} = (1 - \Gamma)I(t) - \left(\lambda + P \frac{R}{d}\right)A(t) \quad (2)$$

where,

$A(t)$ : Cumulative  $^{137}\text{Cs}$  and  $^{210}\text{Pb}_{\text{ex}}$  activity per unit area ( $\text{Bq m}^{-2}$ );

$\Gamma$ : Percentage of the freshly deposited  $^{137}\text{Cs}$  and  $^{210}\text{Pb}$  fallout removed by erosion before being mixed into the plough layer;

$I(t)$ : Annual  $^{137}\text{Cs}$  and  $^{210}\text{Pb}_{\text{ex}}$  deposition flux at time  $t$  ( $\text{Bq m}^{-2} \text{ yr}^{-1}$ );

$\lambda$ : Decay constant for  $^{137}\text{Cs}$  and  $^{210}\text{Pb}_{\text{ex}}$  ( $\text{yr}^{-1}$ );

$P$ : Particle size correction factor;

$R$ : Erosion rate ( $\text{kg m}^{-2} \text{ yr}^{-1}$ );

$d$ : Cumulative mass depth representing the average plough depth ( $\text{kg m}^{-2}$ ).

The  $\Gamma$  is obtained with the formula shown in Eq. 3 (He and Walling 1997), when the  $^{137}\text{Cs}$  and  $^{210}\text{Pb}_{\text{ex}}$  at various soil depths exhibit exponential distribution.

$$\Gamma = P\gamma(1 - e^{-\frac{R}{H}}) \quad (3)$$

where,

$\gamma$ : Proportion of the annual  $^{137}\text{Cs}$  input susceptible to removal by erosion;

$H$ : Relaxation mass depth of the initial distribution of fresh fallout  $^{137}\text{Cs}$  and  $^{210}\text{Pb}_{\text{ex}}$  at the surface of the soil profile ( $\text{kg m}^{-2}$ ).

$A(t)$ , which is  $^{137}\text{Cs}$  inventory at the time of collection, was obtained using Eq. 4 and Eq. 5.

$$A(t) = A(t_0)e^{-\left(\frac{PR}{d} + \lambda\right)(t-t_0)} + \int_{t_0}^t (1 - P\gamma(1 - e^{-R/H}))I(t')e^{-\left(\frac{PR}{d} + \lambda(t-t')\right)} dt' \quad (4)$$

where,  $t_0$  (yr) is the starting time of cultivation.

$A(t_0)$  ( $\text{Bq m}^{-2}$ ), which is the  $^{137}\text{Cs}$  inventory of  $t_0$  (yr), was obtained with the following formula (Eq. 5).

$$A(t_0) = \int_{1954}^{t_0} I(t')e^{-\lambda(t'-t_0)} dt' \quad (5)$$

where,  $A_{\text{ex}}$  is the excess  $^{137}\text{Cs}$  inventory of the sampling point over the reference inventory at year  $t$  ( $\text{Bq m}^{-2}$ ) and  $C_d$  is the  $^{137}\text{Cs}$  concentration of deposited sediment at year  $t'$  ( $\text{Bq kg}^{-1}$ )

This study calculated the soil erosion quantity and redistribution rate using an Excel function developed for easier application of the above formulas (Walling et al. 2007; Zapata 2002). Soil redistribution rate is the sum of soil erosion and sedimentation and, thus, results in (-) and (+) values, which indicate the erosion and sedimentation, respectively. Results of soil redistribution rates were mapped using the GIS software Surfer 12.0 (Golden Software, Golden, Colorado, USA).

## 2.5 Estimation of soil erosion rate using USLE

The amount of annual soil loss at the experimental site was calculated using USLE (Wischmeier and Smith 1978: Eq. 6) with factor values provided by the guidelines of MoE (2012). The rainfall erosivity index ( $R$ ) was  $4111 \text{ MJ} \cdot \text{mm ha}^{-1} \text{ yr}^{-1} \text{ hr}^{-1}$ . The cropping factor ( $C$ ) developed for highland vegetables was 0.4. The conservation practice factor ( $P$ ) was 0.25 for the contour cropping and high ridge cultivation. The soil erodibility factor ( $K$ ) was calculated and used based on the analytical data of each soil sample.

$$A = R \times K \times LS \times C \times P \quad (6)$$

where,

$A$ : Average annual soil loss ( $\text{Mg ha}^{-1} \text{ yr}^{-1}$ );

$R$ : Rainfall erosivity index ( $\text{MJ} \cdot \text{mm ha}^{-1} \text{ yr}^{-1} \text{ hr}^{-1}$ );

$K$ : Soil erodibility factor ( $\text{Mg} \cdot \text{hr MJ}^{-1} \text{ mm}^{-1}$ );

$LS$ : Topographic factor; L is for slope length; S is for slope steepness;

$C$ : Cropping factor;

$P$ : Conservation practice factor.

## 2.6 Statistical analyses

All statistical analyses, including the Pearson correlations, were performed with Minitab 16

software (Minitab Inc., State College, Pennsylvania, USA).

### 3 Results and Discussion

#### 3.1 Spatial distributions of <sup>137</sup>Cs and <sup>210</sup>Pb<sub>ex</sub> in the highland slope

The concentrations of <sup>137</sup>Cs and <sup>210</sup>Pb<sub>ex</sub> within top 10-cm depth at the reference site were in the ranges of 18-21 Bq kg<sup>-1</sup> and 70-210 Bq kg<sup>-1</sup>, respectively. The average concentrations of these radionuclides in the top soil profile (up to 30 cm depth) were 11.57±0.24 Bq kg<sup>-1</sup> and 59.74±4.2 Bq kg<sup>-1</sup>, respectively. The reference site, which was located adjacent to the experimental slope, was the flat area with minimal soil erosion and where no vegetables were cultivated. As shown in Fig. 2, both <sup>137</sup>Cs and <sup>210</sup>Pb<sub>ex</sub> decreased exponentially with soil depth. This result agrees with other reports, which state that <sup>137</sup>Cs and <sup>210</sup>Pb<sub>ex</sub> in soils tends to decrease with soil depth when soil is not disturbed (An et al. 2014; Arata et al. 2018; He and Walling 1997; IAEA 2014; Mabit et al. 2018; Quijano et al. 2016). The concentrations of <sup>137</sup>Cs and <sup>210</sup>Pb<sub>ex</sub> were highest at the 0-5 cm depth. Unlike <sup>210</sup>Pb<sub>ex</sub>, which showed a low concentration below the 10-cm

depth, <sup>137</sup>Cs showed a gradual reduction in rate with depth compared to <sup>210</sup>Pb<sub>ex</sub>. He and Walling (1997) also showed that, with an increase in soil depth, the reduction in <sup>137</sup>Cs concentration was less than that for <sup>210</sup>Pb<sub>ex</sub> in undisturbed soils. This is due to the higher mobility of <sup>137</sup>Cs than <sup>210</sup>Pb<sub>ex</sub> in soil, which results in the facilitated movement of <sup>137</sup>Cs from surface to subsoil (Davis et al. 1984; Dörr and Münnich 1989).

We analyzed concentrations of <sup>137</sup>Cs and <sup>210</sup>Pb<sub>ex</sub> at the middle (B4) and end (B7) sampling points of the slopes (Fig. 1) by taking samples at detailed depths, to compare the spatial-distribution patterns of radionuclides in the soil profile. Spatial distributions of <sup>137</sup>Cs and <sup>210</sup>Pb<sub>ex</sub> in the slope were more heterogeneous than those at the reference site, which is less susceptible to soil erosion than the slope. Fig. 3 shows that distributions of <sup>137</sup>Cs concentrations at different depths varied slightly at the bottom of the slope, but were relatively even (Fig. 3). However, distribution of <sup>210</sup>Pb<sub>ex</sub> at different depths, both in the middle of the slope and at the bottom of the slope, varied more than the <sup>137</sup>Cs distributions, due possibly to erosion or crop cultivation practices. No radionuclide was detected at the soil depth of 28-31 cm at the B4 site, whereas radionuclides were detected at the 50-cm depth at the B7 site. Radionuclide concentration at the 45~50 cm depth at

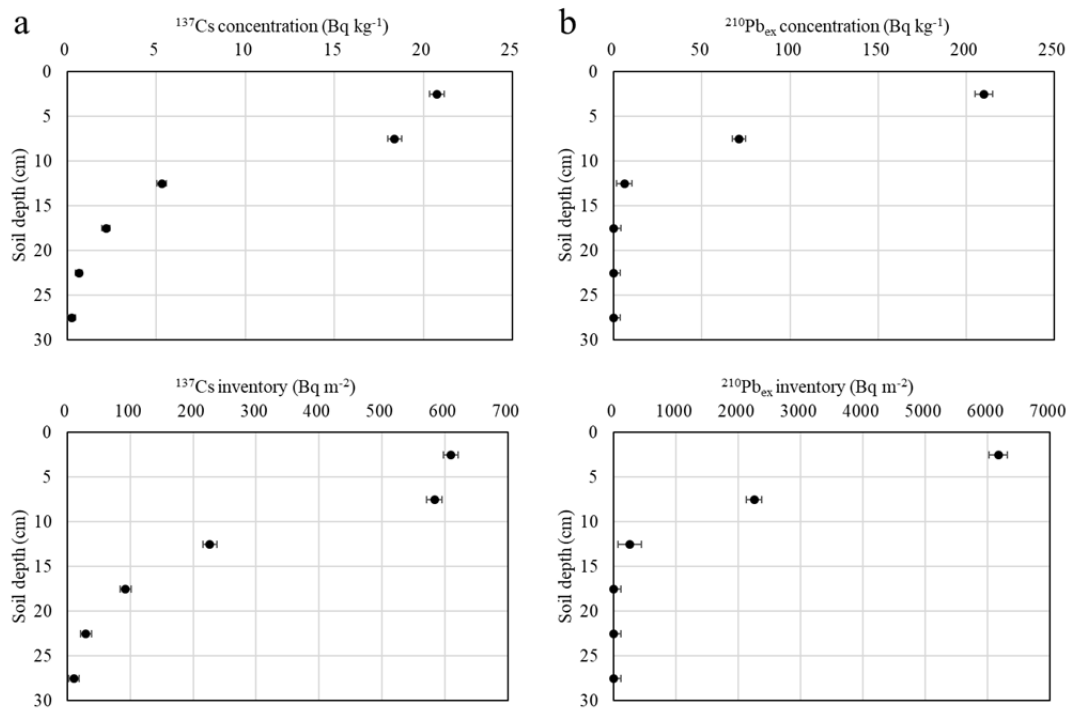
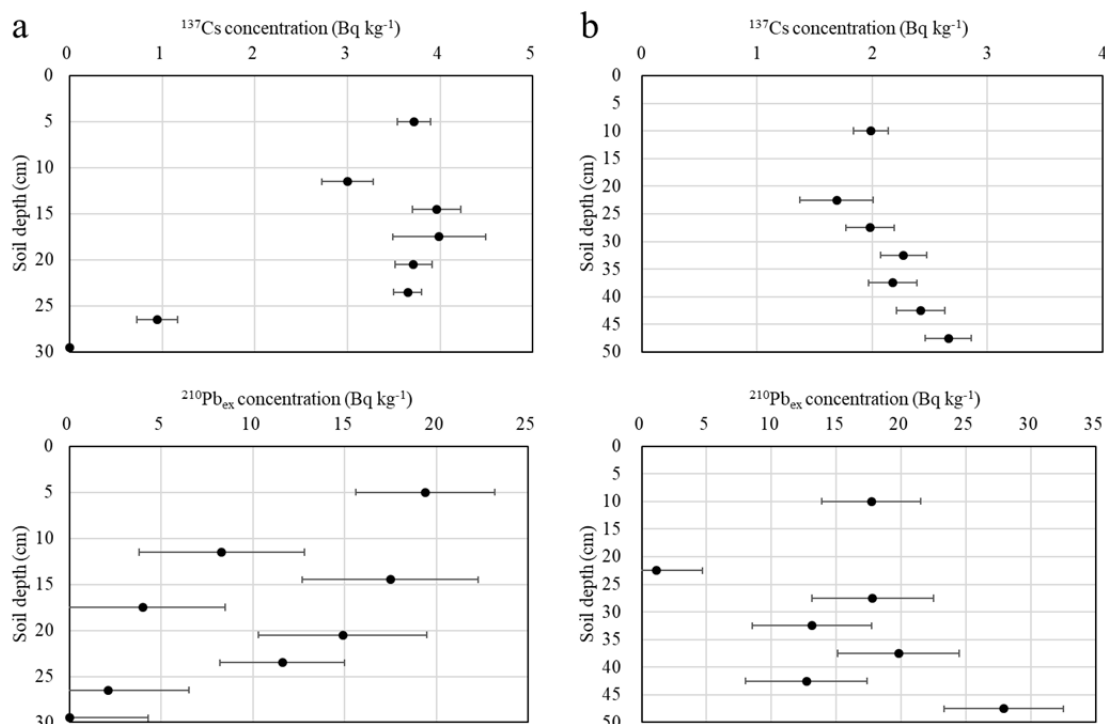
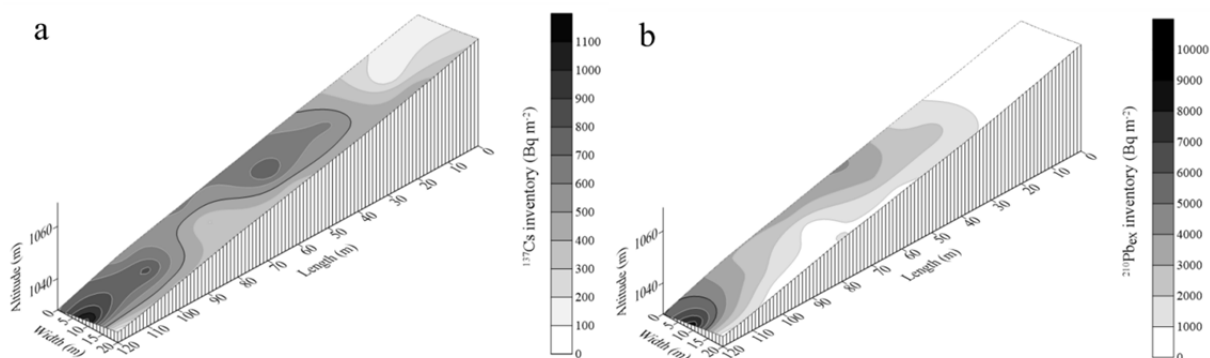


Fig. 2 Distribution of <sup>137</sup>Cs (left) and <sup>210</sup>Pb<sub>ex</sub> (right) concentrations and inventories at different depths at the reference sites where land was an undisturbed flat area near the highland field.



**Fig. 3** Distribution of  $^{137}\text{Cs}$  and  $^{210}\text{Pb}_{\text{ex}}$  concentrations with depth in the Anbandegi highland soil. (a) concentrations at different soil depths (0-10, 10-13, 13-16, 16-19, 19-22, 22-25, 25-28, and 28-30 cm) at the B4 sampling point (middle of the slope), and (b) concentrations at different soil depths (0-20, 20-25, 25-30, 30-35, 35-40, 40-45, and 45-50 cm) at the B7 sampling point (bottom of the slope).



**Fig. 4** Distribution of  $^{137}\text{Cs}$  (a) and  $^{210}\text{Pb}_{\text{ex}}$  (b) inventories across the slope at the Anbandegi highland site ( $n= 21$ ).

B7 was even higher than that of the surface (0~20 cm), indicating that eroded soil particles had accumulated at the bottom of the slope (B7) and that radionuclides moved deep either due to tillage or erosion.

Fig. 4 shows the spatial distribution of the  $^{137}\text{Cs}$  and  $^{210}\text{Pb}_{\text{ex}}$  inventories in the slope that were calculated from their concentrations and the bulk density. As indicated from the analysis of  $^{137}\text{Cs}$  and  $^{210}\text{Pb}_{\text{ex}}$  concentrations in soil (Fig. 2 and 3), distribution of the radionuclide inventories was lower at the starting point of the slope than at the basal

point. For  $^{137}\text{Cs}$ , the inventory of the radionuclides appeared to be high at the center of the slope, for example at the B4 site, and then decreased toward the edges of the slope. The inventory of the radionuclides again increased at B7, but at C7 it was the lowest, possibly due to the higher altitude of C7 than A7 and B7.

The results demonstrated that both concentrations and inventories of  $^{137}\text{Cs}$  and  $^{210}\text{Pb}_{\text{ex}}$  in the fields and reference sites (Fig. 2 and 3) changed with topography and depth, which indicated that

FRNs have a potential to be employed for assessing soil erosion in steep highland areas, where soil has been subjected to intensive soil erosion for several decades.

### 3.2 Relationship of soil physicochemical properties with <sup>137</sup>Cs and <sup>210</sup>Pb<sub>ex</sub>

The relationship between <sup>137</sup>Cs and <sup>210</sup>Pb<sub>ex</sub> concentrations in the experimental field was highly significant ( $p < 0.001$ ) with a slope of 5.87, which indicated that more <sup>210</sup>Pb<sub>ex</sub> existed in the soil than <sup>137</sup>Cs (Fig. 5). He and Walling (1997) and Gasper et al. (2013) showed a similar relationship between <sup>137</sup>Cs and <sup>210</sup>Pb<sub>ex</sub>, which indicated that both radionuclides have similar transport behavior once they are introduced into the soil and combined with soil particles.

The concentrations of <sup>137</sup>Cs and <sup>210</sup>Pb<sub>ex</sub> had significant correlations ( $p < 0.05$ ) with the available phosphorus, organic matter, CEC, and exchangeable cations such as Ca, Mg, and K (Table 2). Mabit and Bernard (1998) reported that <sup>137</sup>Cs concentration showed no correlation with chemical characteristics of a soil, except for organic matter. The highly significant correlation between soil organic matter and concentration distribution of <sup>137</sup>Cs and <sup>210</sup>Pb<sub>ex</sub> in this study reflects the similarity of the spatial distributions of both materials in the soil profile (Table 1; Fig. 2). It showed the tendency of organic matter content to be lower in deeper soil horizons or in areas affected by erosion. It was higher in the top soils which accumulated the radionuclides.

Clay is known to have a strong cohesion with radionuclides (Tamura and Jacobs 1960; Francis and Brinkley 1976; Zapata and Nguyen 2009), but it showed no correlation with radionuclide concentration in this study. Gasper et al. (2013) showed that <sup>137</sup>Cs and <sup>210</sup>Pb<sub>ex</sub> were significantly correlated with organic matter but not with clay content. The negative correlation between clay content and radionuclide concentration might be related to the distribution of clay in the various soil locations on the slope (Table 1) or to the loss of clay in the highly steep slopes that are very vulnerable to soil erosion.

The results revealed that concentration and distribution of <sup>137</sup>Cs and <sup>210</sup>Pb<sub>ex</sub> in the highly steep and erosion-vulnerable highland areas are closely related with soil properties that govern charge characteristics of soil.

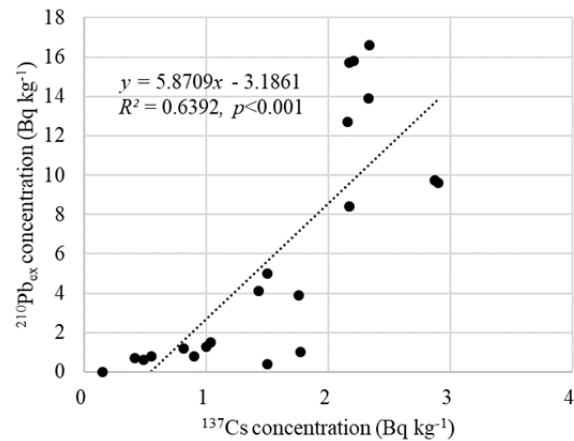


Fig. 5 Relationship between <sup>137</sup>Cs and <sup>210</sup>Pb<sub>ex</sub> concentrations at the Anbandegi highland site ( $n = 21$ ).

Table 2 Pearson correlation coefficients between <sup>137</sup>Cs and <sup>210</sup>Pb<sub>ex</sub> concentrations and soil parameters.

Properties	<sup>137</sup> Cs	<sup>210</sup> Pb <sub>ex</sub>
pH	0.161	0.421
EC	0.174	0.144
Avail-P	0.699***	0.696***
OM	0.724***	0.641**
CEC	0.831***	0.841***
Ca	0.414	0.634**
Mg	0.427	0.647**
K	0.607**	0.754***
Sand	-0.447*	-0.348
Silt	0.556**	0.473*
Clay	-0.051	-0.157

Note: \*, \*\* and \*\*\* indicate significance at the 0.05, 0.01 and < 0.001 levels, respectively.

### 3.3 Soil erosion and redistribution using <sup>137</sup>Cs and <sup>210</sup>Pb<sub>ex</sub>

Measurement of soil erosion in the highly steep, sloped land, where slopes are higher than 30%, is impractical. However, estimation of soil erosion and redistribution is important for conservation measures in the highly sloping lands, because vegetable cultivation is continuing in highlands and erosion causes water pollution downstream of the watershed (Jung et al. 2015; Joo et al. 2004; Lee et al. 2010; MoE 2004, 2012; Park et al. 2011). We employed the FRN method in an effort to estimate soil erosion and redistribution in this highland. Table 3 compares the soil erosion estimated by FRN and USLE. Amount of soil erosion by the FRN method was estimated by the reduction of FRN concentration in the soil as compared to that at the reference site where no erosion takes place.



The average amount of soil erosion from the Anbandegi slopes determined using  $^{137}\text{Cs}$  and  $^{210}\text{Pb}_{\text{ex}}$  were 83.5 and 112.5  $\text{Mg ha}^{-1} \text{yr}^{-1}$ , respectively. A larger amount of soil erosion was assessed with the use of  $^{210}\text{Pb}_{\text{ex}}$  than with  $^{137}\text{Cs}$  (Table 3) due to a higher reduction of  $^{210}\text{Pb}_{\text{ex}}$  concentration in the slope. Concentrations of  $^{137}\text{Cs}$  and  $^{210}\text{Pb}_{\text{ex}}$  remaining in the experimental slope were 16.4 and 10.8%, respectively, of values determined at the reference site. This was also possibly due to  $^{210}\text{Pb}_{\text{ex}}$  being more affected than  $^{137}\text{Cs}$  by recent soil erosion (Gaspar et al. 2013).

**Table 3** Soil erosion rates at the Anbandegi highland site evaluated using  $^{137}\text{Cs}$ ,  $^{210}\text{Pb}_{\text{ex}}$ , and the USLE (Universal Soil Loss Equation) model.

Model	Soil erosion rate ( $\text{Mg ha}^{-1} \text{yr}^{-1}$ )
$^{137}\text{Cs}$	83.5
$^{210}\text{Pb}_{\text{ex}}$	112.5
USLE	166.0 <sup>†</sup> ; 398.3 <sup>‡</sup>

**Note:** <sup>†</sup> calculated with K factor ( $0.0201 \text{ Mg hr MJ}^{-1} \text{ mm}^{-1}$ ) of Cheongryong series (MoE 2012); <sup>‡</sup> calculated with K factor ( $0.0482 \text{ Mg hr MJ}^{-1} \text{ mm}^{-1}$ ) used in this study.

Soil-erosion values estimated by using USLE were 166 to 398  $\text{Mg ha}^{-1} \text{yr}^{-1}$ , and they depended upon which erodibility (K) factor was used. The K values do not account for the rocky fragments in the field currently exposed on the surface of the slope caused by soil erosion. Box (1981) indicated that soil-erosion estimation can be smaller when the K factor is calibrated with rocky fragments (%) in a highly sloping area. Therefore, soil erosion estimation by USLE can be highly variable, depending upon which value of factors in the model are used.

Fig. 6 shows soil redistribution rates that were calculated by using the  $^{137}\text{Cs}$  and  $^{210}\text{Pb}_{\text{ex}}$  data and the mass balance model (Eq. 2~5). Amounts of soil

erosion calculated by distribution of  $^{137}\text{Cs}$  at various points on the slope were in the range of 17.46~207.51  $\text{Mg ha}^{-1} \text{yr}^{-1}$ , whereas those calculated by using  $^{210}\text{Pb}_{\text{ex}}$  were in a wider range of 1.55~581.38  $\text{Mg ha}^{-1} \text{yr}^{-1}$ . Only at the base point of the slope (A7) was 1.55  $\text{Mg ha}^{-1} \text{yr}^{-1}$  accumulated when  $^{210}\text{Pb}_{\text{ex}}$  was used. Altitude at the A7 site is lower than that at the B7 and C7 sites (Fig. 1, 3, and 6), rendering the A7 site to be the outlet of runoff water from the slopes. The redistribution rates that consider both erosion and sedimentation, calculated by  $^{137}\text{Cs}$  and  $^{210}\text{Pb}_{\text{ex}}$ , were all negative values except for the A7 site, indicating erosion prevailed in all areas of the slope. The research site of this study had a 33% slope gradient with no flat areas for sediment accumulation in the slope, which resulted in high overall erosion.

The discrepancy in soil erosion amounts assessed with  $^{137}\text{Cs}$  and  $^{210}\text{Pb}_{\text{ex}}$  might be due to different concentrations of  $^{137}\text{Cs}$  and  $^{210}\text{Pb}_{\text{ex}}$  in the soil. Unlike  $^{137}\text{Cs}$ ,  $^{210}\text{Pb}_{\text{ex}}$  is constantly supplied to soil with rainfall.  $^{137}\text{Cs}$  existed intensively in the atmosphere from 1954 to 1963 but exists, at present, with only a minimal concentration (Zapata 2002; Zapata and Nguyen 2009). This might be a cause for a greater estimation of soil erosion by  $^{210}\text{Pb}_{\text{ex}}$  than  $^{137}\text{Cs}$  (Gaspar et al. 2013). Moreover, the experimental site (Anbandegi) was reclaimed to cultivate vegetables in the late 1960s after global  $^{137}\text{Cs}$  concentration in the atmosphere reached its highest value, and it now has been intensively used for vegetable cultivation for over seven decades. Information on the management practices during those periods are untraceable, but the soil profile might be disturbed due to erosion, tillage, fertilization, and soil dressing (Lee et al. 2010). The decreased fallout of  $^{137}\text{Cs}$  on top soil and changes in soil conditions probably caused the relatively low

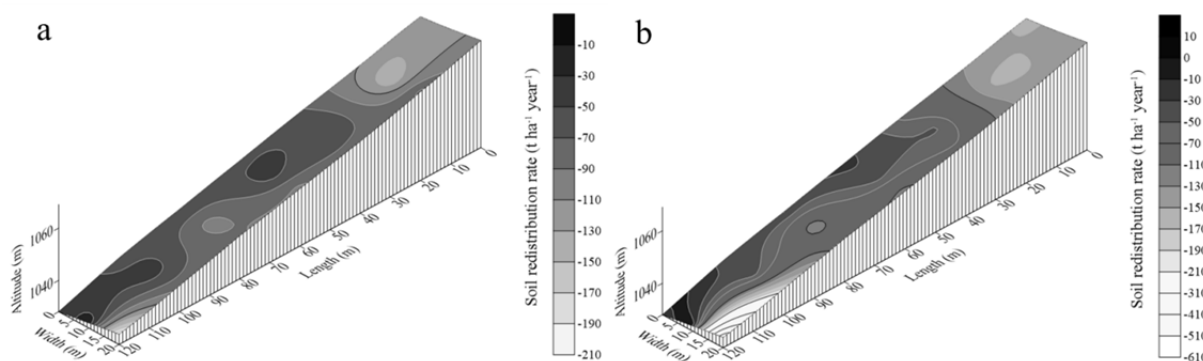


**Fig. 6** Distribution of soil redistribution rates ( $\text{Mg ha}^{-1} \text{yr}^{-1}$ ) estimated using  $^{137}\text{Cs}$  (a) and  $^{210}\text{Pb}_{\text{ex}}$  (b) measurements across the slope at the Anbandegi highland site. Positive values indicate the accumulation of the eroded sediment and negative values stand for the soil erosion.

but even distribution of  $^{137}\text{Cs}$  in the soil profile (Fig. 3). Thus, estimation of soil erosion on the slope by  $^{137}\text{Cs}$  showed less variation than that using  $^{210}\text{Pb}_{\text{ex}}$ .

#### 4 Discussion and Conclusion

Proper estimation of soil erosion on steeply sloping agricultural highlands is a challenging task, but it is an essential step to determine conservation plans for soil and water. This study demonstrated the feasibility of using the  $^{137}\text{Cs}$  and  $^{210}\text{Pb}_{\text{ex}}$  FRN method to assess spatial variations of soil erosion and redistribution on a steep slope. Soil physicochemical properties (Table 1), inventories, spatial distributions of  $^{137}\text{Cs}$  and  $^{210}\text{Pb}_{\text{ex}}$  at specific points along the slope (Fig. 1, 2, 3, and 4), and spatial variability of soil erosion and redistribution (Fig. 6; Table 3) were analyzed. Changes in soil properties and concentrations of  $^{137}\text{Cs}$  and  $^{210}\text{Pb}_{\text{ex}}$  at specific points along the slope showed that large amounts of soil were eroded. Variations in soil-erosion amounts measured by  $^{137}\text{Cs}$ ,  $^{210}\text{Pb}_{\text{ex}}$ , and USLE were large, as expected, and, thus, this necessitates verification to determine which estimate represents erosion on the very steep slope. A significant correlation existed between  $^{137}\text{Cs}$  and  $^{210}\text{Pb}_{\text{ex}}$  concentrations on the slope, but reduction rates of  $^{210}\text{Pb}_{\text{ex}}$  were higher than those for  $^{137}\text{Cs}$  (Fig. 5), which caused estimates of erosion using  $^{210}\text{Pb}_{\text{ex}}$  to be higher than those using  $^{137}\text{Cs}$ .

Verification of soil-erosion values using the USLE model and the FRN method has been controversial (Gaspar et al. 2013; Gharibreza et al. 2021; Mabit et al. 2002, 2018; Ni et al. 2018; Walling et al. 2007; Saç et al. 2008). Erosion values from both methods have an inherent limitation, because of the need to prove which values should be accepted. Saç et al. (2008) verified the suitability of using the  $^{137}\text{Cs}$  method, as it had a good correlation with USLE estimates. Soil-erosion measurements should be made at several research sites, and they may need to consider both water and wind erosion. Gaspar et al. (2013) demonstrated the potential for coupling  $^{210}\text{Pb}_{\text{ex}}$  and  $^{137}\text{Cs}$  measurements for assessing soil redistribution in Mediterranean environments at different temporal scales, and they suggested a need for further studies to solve uncertainties associated with the application of  $^{210}\text{Pb}_{\text{ex}}$  in highly heterogeneous environments, such as was found in Mediterranean mountains. Mabit et al. (2002) reported that the net production of sediment

estimated from  $^{137}\text{Cs}$  data was greater than that measured at the outlet by the GAMES model (using USLE), and they suggested several advantages of FRN methods over other soil erosion models. Gharibreza et al. (2021) stated that the RUSLE model overestimated erosion rates, as compared to those determined by  $^{137}\text{Cs}$  measurements, and a perfect agreement would not be expected between the two methods. Ni et al. (2017) found consistent, linear relationships between  $^{137}\text{Cs}$  content and inter-gully erosion. Walling et al. (2007) proved the potential use of  $^{137}\text{Cs}$  measurements for estimation of rates and spatial patterns of erosion and deposition, and they used this information for testing and validation of other soil erosion models.

It is not possible to distinguish between the FRN and USLE methods to determine which one estimates better soil erosion, because the USLE model provides an average annual erosion loss (Table 3). But the FRN method can provide soil erosion ranges and give values for spatial erosion and redistribution at specific sites (Fig. 2, 3, 4 and 6). Thus, correlation of soil erosion determined by using the USLE and FRN methods requires extensive field measurements, which were not feasible in this study.

The FRN method, which measures soil erosion at specific points in a field, seems to have an advantage over the USLE model, because site-specific data from FRNs can provide the rate and spatial pattern of erosion and deposition in a field. These data are useful in setting protocol for best management practices (BMP) for soil-erosion control. The USLE model provides an estimate of soil loss by water but does not account for sediment deposition. However, verification of soil-erosion values using the FRN method in steeply sloping highlands merits further study at many locations with different soils, topography, and management practices.

In steeply sloping agricultural highlands, it is critical to estimate the net sediment production, the spatial variability of soil redistribution, and the origin of the exported sediments rather than just to estimate an annual average amount of soil erosion in a field (An et al. 2014; Ascough II et al. 2018; Gaspar et al. 2013; IAEA 2014; Mabit et al. 2002, 2018; Meusburger et al. 2020; Walling et al. 2007). Amounts of soil erosion calculated with  $^{137}\text{Cs}$  and  $^{210}\text{Pb}_{\text{ex}}$  are based on concentration changes during the past 50 years and 100 years, respectively, times which consider the occurrence and fate of the radionuclides

(He and Walling 1997; Walling et al. 2007). Also, the FRN method considers not only water and wind erosion but also management practices such as tillage (Gharibreza et al. 2021). However, USLE, in its estimation of soil loss, does not account for such long-term changes in a field. In addition, the USLE model is not suitable for estimating soil erosion in steeply sloping soil. A perfect correlation between the FRN and USLE models is not to be expected (Gharibreza et al. 2021).

Based on the results from this study, as well as other studies, we conclude that the FRN method using  $^{137}\text{Cs}$  and  $^{210}\text{Pb}_{\text{ex}}$  radionuclides can be used to assess soil erosion and redistribution in steeply sloping

agricultural highlands where a long-term crop cultivation causes large amounts of soil erosion to occur.

## Acknowledgement

This research was supported in part by Research Grant from Kangwon National University (No. 520160156: 2016) and by the Korea Ministry of Environment, with the strategic EcoSSoil Project, KEITI (Korea Environmental Industry and Technology Institute), Korea (Grant No. 2019002820004).

## References

- An J, Zheng F, Wang B (2014) Using  $^{137}\text{Cs}$  technique to investigate the spatial distribution of erosion and deposition regimes for a small catchment in the black soil region, Northeast China. *Catena* 123:243-251. <https://doi.org/10.1016/j.catena.2014.08.009>
- Arata L, Meusburger K, Frenkel E, et al. (2016) Modelling deposition and erosion rates with radionuclides (MODERN)-Part 1: A new conversion model to derive soil redistribution rates from inventories of fallout radionuclides. *J Environ Radioactivity* 162-163:45-55. <https://doi.org/10.1016/j.jenvrad.2016.05.008>
- Arnold JG, Srinivasan R, Muttiah RS, et al. (1998) Large area hydrologic modelling and assessment Part I: Model development. *J Am Water Resour Assoc* 34:73-89. <https://doi.org/10.1111/j.1752-1688.1998.tb05961.x>
- Ascough II JC, Flanagan DC, Tatarko J, et al. (2018) Soil erosion modelling and conservation planning. In Delgado et al. (ed.) *Precision Conservation: Geospatial techniques for agricultural and natural resources conservation*. Agronomy Monograph 59, American Society of Agronomy, Crop Science Society of America and Soil Science Society of America, Madison, WI, USA.
- Box JE (1981) The effects of surface slaty fragments on soil erosion by water. *Soil Sci Soc Am J* 45(1):111-116. <https://doi.org/10.2136/sssaj1981.03615995004500010024x>
- Bray RH, Kurtz LT (1945) Determination of total, organic, and available forms of phosphorus in soils. *Soil Sci* 59(1):39-46. <https://doi.org/10.1097/00010694-194501000-00006>
- Croke J, Nethery M (2006) Modelling runoff and soil erosion in logged forests: Scope and application of some existing models. *Catena* 67(1):35-49. <https://doi.org/10.1016/j.catena.2006.01.006>
- Davis RB, Hess CT, Norton SA, et al. (1984)  $^{137}\text{Cs}$  and  $^{210}\text{Pb}$  dating of sediments from soft-water lakes in New England (U.S.A.) and Scandinavia: a failure of  $^{137}\text{Cs}$  dating. *Chem Geol* 44:151-181. [https://doi.org/10.1016/0009-2541\(84\)90071-8](https://doi.org/10.1016/0009-2541(84)90071-8)
- Dörr H, and Münnich KO (1989) Downward movement of soil organic matter and its influence on trace-element transport ( $^{210}\text{Pb}$  and  $^{137}\text{Cs}$ ) in the soil. *Radiocarb* 31:655-663. <https://doi.org/10.1017/S003382220001225x>
- Elliott GL, Campbell BL, Loughran RJ (1990) Correlation of erosion measurement and soil caesium-137 content. *Inr J Radiat Appl Instrum Part A Appl Radiat Isot* 41:713-717. [https://doi.org/10.1016/0883-2889\(90\)90017-B](https://doi.org/10.1016/0883-2889(90)90017-B)
- Flanagan DC, Gilley JE, Franti TG (2007) Water Erosion Prediction Project (WEPP): Development, history, model capabilities, and future enhancements. *Trans ASABE* 50:1603-1612. <https://doi.org/10.13031/2013.23968>
- Francis CW, Brinkley FS (1976) Preferential adsorption of  $^{137}\text{Cs}$  to micaceous minerals in contaminated freshwater sediment. *Nature* 260(5551):511-513. <https://doi.org/10.1038/260511a0>
- Gaspar L, Navas A, Walling DE, et al. (2013) Using  $^{137}\text{Cs}$  and  $^{210}\text{Pb}_{\text{ex}}$  to assess soil redistribution on slopes at different temporal scales. *Catena* 102:46-54. <https://doi.org/10.1016/j.catena.2011.01.004>
- Gharibreza M, Samani AB, Arabkhedri M, et al. (2021) Investigation of on-site implications of tea plantations on soil erosion in Iran using  $^{137}\text{Cs}$  method and RUSLE. *Environ Earth Sci* 80(1):1-14. <https://doi.org/10.1007/s12665-020-09347-y>
- He Q, Walling DE. (1997) The distribution of fallout  $^{137}\text{Cs}$  and  $^{210}\text{Pb}$  in undisturbed and cultivated soils. *Appl Radiat Isot* 48(5):677-690. [https://doi.org/10.1016/S0969-8043\(96\)00302-8](https://doi.org/10.1016/S0969-8043(96)00302-8)
- International Atomic Energy Agency (IAEA). (2014) Guidelines for using fallout radionuclides to assess erosion and effectiveness of soil conservation strategies. Joint FAO/IAEA Programme, IAEA TECDOC Series IAEA-TECDOC-1741, IAEA, Vienna, Austria.
- Joo JH, Park C, Jung YS, et al. (2004) Evaluation of the dressed soil applied in mountainous agricultural land. *Korean J Soil Sci Fert* 37:245-250.
- Jung KH, Kim WT, Hur SO, et al. (2004) USLE/RUSLE factors for national scale soil loss estimation based on the digital detailed soil map. *Korean J Soil Sci Fert* 37(4):199-206.
- Jung YH, Kum DH, Han JH, et al. (2015) Study on Topsoil Erosion Indices for Efficient Topsoil Management. *J Korean Soc Water Environ* 31(5):543-555.
- Karydas CG, Panagos P, Gitas IZ (2012) A classification of water erosion models according to their geospatial characteristics. *Int J Digit Earth* 7(3):229-250. <https://doi.org/10.1080/17538947.2012.671380>
- Lee GJ, Lee JT, Ryu JS, et al. (2010) Status and soil management problems of highland agriculture of the main mountainous region in the South Korea. *Proceedings of the 19th World Congress of Soil Science, Soil Solutions for a Changing World 1 - 6 August 2010, Brisbane, Australia*, pp 154-157.

- Mabit L, Klik A, Benmansour M, et al. (2009) Assessment of erosion and deposition rates within an Austrian agricultural watershed by combining  $^{137}\text{Cs}$ ,  $^{210}\text{Pb}_{\text{ex}}$  and conventional measurements. *Geoderma* 150(3):231-239. <https://doi.org/10.1016/j.geoderma.2009.01.024>
- Mabit L, Benmansour M, Abril JM, et al. (2014) Fallout  $^{210}\text{Pb}$  as a soil and sediment tracer in catchment sediment budget investigations: A review. *Earth-Sci Rev* 138: 335-351. <http://dx.doi.org/10.1016/j.earscirev.2014.06.007>
- Mabit L, Bernard C (1998) Relationship between soil  $^{137}\text{Cs}$  inventories and chemical properties in a small intensively cropped watershed. *C r Acad sci, Ser 2, Earth planet sci* 327(8):527-532. [https://doi.org/10.1016/S1251-8050\(99\)80034-2](https://doi.org/10.1016/S1251-8050(99)80034-2)
- Mabit L, Bernard C, Laverdière MR (2002) Quantification of soil redistribution and sediment budget in a Canadian watershed from fallout caesium-137 ( $^{137}\text{Cs}$ ) data. *Can J Soil Sci* 82(4):423-431. <https://doi.org/10.4141/s02-016>
- Mabit L, Bernard C, Yi ALZ, et al. (2018) Promoting the use of isotopic techniques to combat soil erosion: An overview of the key role played by the SWMCN Subprogramme of the Joint FAO/IAEA Division over the last 20 years. *Land Degrad Dev* 29:3077-3091. <https://doi.org/10.1002/ldr.3016>
- Mabit L, Benmansour M, Walling DE (2008) Comparative advantages and limitations of the fallout radionuclides  $^{137}\text{Cs}$ ,  $^{210}\text{Pb}_{\text{ex}}$  and  $^7\text{Be}$  for assessing soil erosion and sedimentation. *J Environ Radioact* 99(12):1799-1807. <https://doi.org/10.1016/j.jenvrad.2008.08.009>
- Meusburger K, Mabit L, Park JH, et al. (2013) Combined use of stable isotopes and fallout radionuclides as soil erosion indicators in a forested mountain site, South Korea. *Biogeosciences* 10(8):5627-5638. <https://doi.org/10.5194/bg-10-5627-2013>
- Meusburger K, Evrard O, Alewell C, et al. (2020) Plutonium aided reconstruction of caesium atmospheric fallout in European topsoils. *Sci Rep* 10:11858. <https://doi.org/10.1038/s41598-020-68736-2>
- Miller WP, Miller DM (1987) A micro-pipette method for soil mechanical analysis. *Comm Soil Sci Plant Anal* 18(1):1-15. <https://doi.org/10.1080/00103628709367799>
- Ministry of Environment (MoE) (2004) Comprehensive plan for reducing non-point pollution in highland areas. Ministry of Environment, Korea.
- Ministry of Environment (MoE) (2012) The Notice about the Erosion Status Survey and Measures such as Topsoil. Ministry of Environment, Korea. pp. 1-26.
- Morgan RPC, Quinton JN, Rickson RJ (1990) Structure of the Soil Erosion Prediction Model for the European Community. In: Proceedings of International Symposium on Water Erosion, Sedimentation and Resource Conservation, Dehradun.
- Nearing MA, Forster GR, Lane LJ (1989) A Process-based Soil Erosion Model for USDA Water Erosion Prediction Project. *Trans ASAE* 32:1587-1593. <https://doi.org/10.13031/2013.31195>
- Nelson DW, Sommers LE. (1996) Total carbon, organic carbon, and organic matter. In Sparks DL et al. (eds.). *Methods of Soil Analysis. Part 3. Chemical Methods. Soil Science Society of America, Inc, and American Society of Agronomy, Madison, WI, USA*, pp 961-1010.
- Ni LS, Fang NF, Shi ZH, et al. (2017) Validating a basic assumption of using cesium - 137 method to assess soil loss in a small agricultural catchment. *Land Degrad Dev* 28(5):1772-1778. <https://doi.org/10.1002/ldr.2708>
- Park CS, Jung YS, Joo JH, et al. (2004) Soil Characteristics of the Sapprolite Piled Upland Fields at Highland in Gangwon Province. *Korean J Soil Sci Fert* 37(2):66-73.
- Park SY, Oh CY, Jeon SW, et al. (2011) Soil Erosion Risk in Korean Watersheds, Assessed Using the Revised Universal Soil Loss Equation. *J Hydrol* 399(3):263-273. <https://doi.org/10.1016/j.jhydrol.2011.01.004>
- Quijano L, Beguería S, Gaspar L, et al. (2016) Estimating erosion rates using  $^{137}\text{Cs}$  measurements and WATEM/SEDEM in a Mediterranean cultivated field. *Catena* 138:38-51. <https://doi.org/10.1016/j.catena.2015.11.009>
- Rabesiranana N, Rasolonirina M, Solonjara AF, et al. (2016) Assessment of soil redistribution rates by  $^{137}\text{Cs}$  and  $^{210}\text{Pb}_{\text{ex}}$  in a typical Malagasy agricultural field. *J Environ Radioact* 152:112-118. <https://doi.org/10.1016/j.jenvrad.2015.11.007>
- Renard KG, Foster GR, Weesies GA, et al. (1997) Predicting Soil Erosion by Water: a Guide to Conservation Planning with the Revised Universal Soil Loss Equation (RUSLE), Agriculture Handbook, Washington, p 703.
- Ritchie JC, McHenry JR (1990) Application of radioactive fallout cesium-137 for measuring soil erosion and sediment accumulation rates and patterns: a review. *J Environ Qual* 19(2):215-233. <https://doi.org/10.2134/jeq1990.00472425001900020006x>
- Saç MM, Uğur A, Yener G, et al. (2008) Estimates of soil erosion using cesium-137 tracer models. *Environ Monit Assess* 136:461-467. <https://doi.org/10.1007/s10661-007-9700-8>
- Sumner ME, Miller WP (1996) Cation exchange capacity and exchange coefficients. In D.L. Sparks AL et al. (eds.). *Methods of Soil Analysis. Part 3. Chemical Methods. Soil Science Society of America, Inc, and American Society of Agronomy, Madison, WI, USA*, pp. 1201-1229.
- Tamura T, Jacobs DG (1960) Structural implications in cesium sorption. *Health physics* 2(4):391-398. <https://doi.org/10.1097/00004032-195910000-00009>
- Walling DE, Zhang Y, He Q (2007). Models for converting measurements of environmental radionuclide inventories ( $^{137}\text{Cs}$ , Excess  $^{210}\text{Pb}$ , and  $^7\text{Be}$ ) to estimates of soil erosion and deposition rates (including software for model implementation). Including Software for Model Implementation. [www-naweb.iaea.org/nafa/swmn/Helpfile.pdf](http://www-naweb.iaea.org/nafa/swmn/Helpfile.pdf) (accessed on 20 August 2021)
- Wischmeier WH, Smith DD (1978) Predicting rainfall erosion losses-a guide to conservation planning. *Agric. Handbook No. 537*, U.S. Gov. Print. Office, Washington, DC, USA.
- Zapata F (2002) Handbook for the Assessment of Soil Erosion and Sedimentation using Environmental Radionuclides. Kluwer Ac. Publ., Dordrecht, Netherlands, p 219.
- Zapata F, Nguyen ML (2009) Soil erosion and sedimentation studies using environmental radionuclides. *Radioact Environ* 16:295-322. [https://doi.org/10.1016/S1569-4860\(09\)01607-6](https://doi.org/10.1016/S1569-4860(09)01607-6)